CONF 8808146--1

To be publ. in Proc. of 10th International Conf. on Free Electron Lasers, Israel 1988 Aug. 29 - Sept. 2, 1988
Jerusalem

FREE ELECTRON LASER WITH SMALL PERIOD WIGGLER AND SHEET ELECTRON BEAM: A STUDY OF THE FEASIBILITY OF OPERATION AT 300 GHz WITH 1 MW CW OUTPUT POWER

J.H. Booske, V.L. Granatstein, T.M. Antonsen, Jr., W.W. Destler, J. Finn
P.E. Latham, B. Levush, I.D. Mayergoyz, D. Radack, and J. Rodgers
Laboratory for Plasma Research
University of Maryland
College Park, MD 20742-3511, USA

CONF-8808146--17
DE89 014759

M.E. Read and A. Linz
Physical Sciences, Inc.
Arlington, VA 22314, USA

ABSTRACT

The use of a small period wiggler ($\ell_w < 1$ cm) together with a sheet electron beam has been proposed as a low cost source of power for electron cyclotron resonance heating (ECRH) in magnetic fusion plasmas. Other potential applications include space-based radar systems. We have experimentally demonstrated stable propagation of a sheet beam (18 A, 1 mm × 20 mm) through a ten-period wiggler electromagnet with peak field of 1.2 kG. Calculation of microwave wall heating and pressurized water cooling have also been carried out, and indicate the feasibility of operating a near-millimeter, sheet beam FEL with an output power of 1 MW CW (corresponding to power density into the walls of 2 kW/cm^2). Based on these encouraging results, a proof-of-principle experiment is being assembled, and is aimed at demonstrating FEL operating at 120 GHz with 300 kW output power in 1 μs pulses; electron energy would be 410 keV. Preliminary design of a 300 GHz, 1 MW FEL with an untapered wiggler is also presented.

FG05-87ER52147

+B

I. INTRODUCTION

Following the discovery[1] of a simple and adjustable electromagnet configuration for short period wigglers ($\ell_w < 1$ cm where ℓ_w is the wiggler period length) with strong magnetic field amplitudes, a research program was initiated at the University of Maryland to determine the feasibility of developing free electron laser (FEL) oscillators which would require relatively modest electron energy. As described in Ref. [2], the resulting proposed concept is characterized by a sheet electron beam with $V_{beam} < 1$ MeV, a thermionic electron gun, the short period wiggler, and a depressed collector for spent beam energy recovery. The FEL is designed to operate in the millimeter wave regime (frequency approaching 300 GHz), and to be compatible with CW operation.

In this paper we will describe a self-consistent design procedure for low gain untapered FEL oscillators, identify critical feasibility issues, present results of studies addressing two of these issues, and discuss future plans. The oscillator design procedure is presented in Section II, feasibility issues are discussed in Section III, and our near-term future research objectives are outlined in Section IV.

II. DESIGN OF LOW-GAIN UNTAPERED FEL OSCILLATORS

In this section we describe a planar wiggler FEL oscillator design process which is a generalization of the optimized FEL oscillator design process (for untapered wigglers) described in Ref. [3]. As shown in the previous work, when wiggler parameters are constant over the entire interaction length, the single-pass, single electron FEL dynamics for low-gain systems can be written as

$$\frac{d\psi}{d\xi} = \mathcal{P} \tag{1}$$

$$\frac{d\mathcal{P}}{d\xi} = -\mathcal{A}\sin\psi \tag{2}$$

where

$$\mathcal{P} \equiv \frac{\omega L}{c}\frac{\delta\gamma}{(\gamma_R\beta_R)^3}, \tag{3}$$

$$\mathcal{A} \equiv \left(\frac{\omega L}{c}\right)^2 \frac{a_w a_s}{(\gamma_R \beta_R)^4}, \tag{4}$$

$\gamma = (1-\beta^2)^{-1/2} = \gamma_R + \delta\gamma$, $a_w = eA_w/mc^2$, $a_s = eAs/mc^2$, $\xi = z/L$, $\phi = (k_w + k_s)z - \omega t$. $\beta = v/c$ is the beam velocity normalized to the speed of light, A_w and A_s are the wiggler and radiation magnetic vector potential amplitudes, respectively. L is the interaction length. $k_w = 2\pi/\ell_w$ and γ_R and β_R are the resonant normalized energy and velocity for which $\beta_R c = \omega/(k_w + k_s)$. We refer to the normalized quantity $\mathcal{P}$ as the universal FEL electron energy (it is also the normalized detuning parameter) and to $\mathcal{A}$ as the universal beat wave potential amplitude.[3] Equations(1)-(4) were derived under the assumption of weakly perturbed electron orbits for which $a_w^2 \ll 1$. More general equations are presented and discussed in [4].

Equations (1) and (2) are the single electron equations of motion which are solved for the universal efficiency $\Delta\mathcal{P} \equiv \mathcal{P}_{inj} - \mathcal{P}(\xi = 1)$ as a function of $\mathcal{A}$ and $\mathcal{P}_{inj}$ ($\mathcal{P}_{inj}$ is the value of $\mathcal{P}$ at $\xi = 0$). To model the effects of an electron beam. $\Delta\mathcal{P}$ is averaged over N discrete electrons representing a uniform phase distribution at injection,

$$< \Delta\mathcal{P} >_N = \mathcal{P}_{inj} - < \mathcal{P}(1) >_N . \tag{5}$$

In addition to this calculation of $< \Delta\mathcal{P} >_N$, two other pieces of information are necessary. The first is to characterize the many possible equilibrium oscillator states in terms of beam current. Specifically, we have found it convenient to do this in terms of a normalize parameter $\chi = I_{beam}/I_{start}$, where I_{start} is the start oscillation current. The other required item is to identify under what conditions one can theoretically expect a candidate equilibrium state to exhibit stable, single-mode operation. This information has been determined from solving the equations of motion [i.e. Eqs. (1) and (2)] simultaneously with the time-dependent wave equation, allowing for the existence of multiple (axial) cavity modes.[5]

The final result of these calculations has been summarized in Fig. 1. The vertical and horizontal axes represent $\mathcal{P}_{inj}$ and $\mathcal{A}$, respectively. The solid lines are contours of constant universal efficiency $< \Delta\mathcal{P} >_N$, and the dashed lines represent equilibrium states parameterized by constant values of $\chi = I_{beam}/I_{start}$. The dotted line represents a stability boundary.[6] Points within the triangular-shaped stability region correspond to stable, single-mode equilibria. Note from Fig. 1 that to operate a low gain CW FEL oscillator at single frequency with maximum efficiency, the electron beam current must be roughly three times the maximum start oscillation current ($\chi \approx 3$). Furthermore, the time-dependent multi-mode simulations have identified that, in general, finite voltage pulse risetime effects will most likely result in the majority of low-gain FEL oscillators operating along the upper boundary of the stability region.[7] Additional details of these simulations are presented in the paper by B. Levush and T.M. Antonsen, Jr., in this journal issue.

The next step requires converting dimensionless quantities selected from Fig. 1 into dimensional device specifications. This is accomplished by deriving scaling laws which relate the relevant dimensionless and dimensional parameters. Most of the derivation steps are described in Ref. [3], and thus, we have just summarized the most important scaling relations below in Table I.

An example of using the universal operating map of Fig. 1 along with the scaling relations to design untapered FEL oscillators is manifested in our previously described 1.0 MW, 300 GHz conceptual design.[3] For this exercise, a device with optimized efficiency was desired. Looking at Fig. 1, the highest universal efficiency achievable with a stable single-mode equilibrium has a value of $< \Delta\mathcal{P} >_N \approx 5.3$, with $\chi \approx 3, \mathcal{P}_{inj} \approx 5.5$, and $\mathcal{A} \approx 15$. Substituting these quantities into the relations of Table I along with a choice of wiggler length L, the desired frequency, and the output power yields the design parameters listed in the leftmost column of Table II. As seen in the table, this proposed FEL system should yield the 1.0 MW output at 300 GHz with a 500 kV beam and a 5.4 mm wiggler period. The intrinsic efficiency is approximately 5% and CW operation would require the dissipation of approximately 2 kW/cm^2 of ohmic radiation losses in the cavity walls.[3]

III. FEASIBILITY ISSUES

There are several very important feasibility issues to address before the short period wiggler FEL oscillator can be characterized as a viable alternative for efficient generation of high power millimeter wave radiation. This is especially true for applications requiring CW operation. A list of the most important issues includes: (1) the feasibility of designing 500 kV, CW, sheet electron beam guns that are voltage tunable, (2) the feasibility of designing broadband (or tunable) oscillator cavities that are compatible with tightly constrained geometry and unimpeded beam propagation; (3) the feasibility of designing depressed collectors for energy recovery from 500 kV sheet electron beams; (4) the feasibility of propagating sheet electron beams down the narrow cavity gap between the two wiggler magnet halves while avoiding excessive beam interuption; and, (5) the feasibility of dissipating large heat fluxes in the cavity walls resulting from radiation ohmic losses. At this point in our research program, items (1), (2) and (4) are the subjects of ongoing investigations. Item (5) was the subject of a recently completed study, while a study of item (3) will be an issue for future consideration if the results of studying the other four issues as well as conducting planned FEL experiments yield a positive judgment for our concept. Below, we summarize our findings to date on items (4) and (5).

A. Propagation of Wiggler-Focused Sheet Electron Beams

The dominant concern here is whether one can propagate up to 20 MW of 500 kV, wiggler-focused, sheet beam power down a narrow cavity gap (small transverse dimension = 2.2 mm, cf. Table II), with negligible loss of beam power (i.e., less than approximately 0.5%) to the walls. To address this question, both experimental and theoretical investigations are being pursued. For example, a theoretical simulation of beam transport based on numerical particle orbit calculations is about to commence. These simulations should predict what beam quality at injection is required to avoid current loss to the cavity walls. Effects such as wiggler entrance tapers and field errors, space charge, and cavity radiation fields will be considered. To complement the theoretical studies, a series of wiggler-focused sheet electron beam propagation experiments are in progress. Our first results using a five-period wiggler magnet with a 1.0 cm wiggler period have been previously published.[8]. Similar measurements using a ten-period magnet (also with a 1.0 cm period) and a 1 mm × 20 mm sheet beam are presently underway. Preliminary results achieved with approximately 18 A of beam current have been very promising. In fact, as seen in Fig. 2, nearly 100% beam current transmission has been observed within the measurement accuracy for these ten-period wiggler experiments. This result, which is an improvement over the previous results achieved with the five-period wiggler,[8] is attributed to improvements in the wiggler field entrance conditions. Furthermore, in no instance have we experimentally observed any evidence for beam breakup or filamentation-type instabilities.

B. Thermal Analysis of Ohmic Wall Losses

To determine technological limits on ohmic heat flux that could be stably dissipated in the cavity walls, a numerical simulation was conducted. The analysis was performed using the code "supersap", which is a finite element code capable of modeling 2-D transient heat transfer problems.

The analysis was done using the geometry of Fig. 3. The electromagnet was modeled as alternating slabs of copper and silicon steel, each with a thickness of 1.25 mm. The depth of the slabs was 5 cm. At the bottom of the slabs was a 0.25 mm thick copper layer, representing the cavity wall. Cooling channels were placed in the copper slabs. Note that this configuration assumes a thermally conducting, but electrically insulating interface between the magnet and cavity wall. Such an interface would be accomplished by a thin diamond film layer or similar material. Alternatively, the electromagnet might be replaced with a permanent magnet if magnetic materials can be found which yield the necessary field strengths in these short period wigglers.

For the modeling, it was assumed that there was a constant, uniform flux of 1000, 1500, or 2000 W/cm^2 at the surface of the waveguide wall. Admittedly, for an oscillator there will be a standing wave pattern in the axial direction. The scale length of this pattern, however, will be one-half the wavelength, or 0.5 mm for a 300 GHz device. This is somewhat smaller than the scale length of thermal diffusion in the structure, and thus the assumption of uniform heat load is expected to be an acceptable approximation.

Figure 4 shows a typical evolution of the temperatures at several representative locations in the structure. The significance of these data is that for time intervals greater than approximately 1.0 sec, the heat transfer is essentially a steady state problem.

Numerous cases were simulated for the different heat fluxes specified above (in all cases, the coolant was considered to be pressurized water). The final results for the maximum temperatures over the whole structure and at the cooling channels are plotted in Fig. 5. In all cases, the maximum temperature is less than 300° C, the temperature at which material deformation in copper becomes a concern. Since the analysis assumed a heat transfer based on water in the liquid phase, these elevated temperatures mandate the coolant to be under static pressure to avoid boiling in the cooling channels. For the three heat fluxes, the static pressures required are listed in Table III. Clearly, the static pressure necessary for 1000 W/cm^2 is negligible. For 1500 W/cm^2, 44 psig is required, which would raise the maximum system pressure to 165 psig (this includes the dynamic pressure required to overcome friction losses in the channels). No power is expended in producing the static load, however, so this is almost certainly acceptable. The 210 psig required for 2000 W/cm^2 is probably also acceptable, but requires careful thought.

The conclusion to this analysis is that thermal heat fluxes up to – but probably not much above – 2000 W/cm^2 may be safely handled in the short period wiggler FEL. It was considered that this analysis was conservative to the extent that sophisticated cooling techniques – such as nucleate boiling – were not required. Nucleate boiling is often used as a cooling mechanism, and could extend the limits calculated here. It is noted that 1000 W/cm^2 is often considered an upper limit to cooling of large areas in microwave tubes. For smaller areas, such as cavities in gyrotron oscillators, thermal loads in excess of 2 kW/cm^2 have been handled.[9] The calculations carried out here are consistent with the surface area being intermediate in size.

FUTURE PLANS

Our future research plans include theoretical and experimental studies of short period wiggler FEL oscillators. A proof-of-principle (PoP) experiment at 120 GHz is entering a construction phase. This device will utilize a SLAC klystron thermionic Pierce diode with a graphite/molybdenum mask to produce a sheet beam. The diode will be pulsed with a 450 kV, 1 μs voltage pulse obtained with the University of Maryland's 200 MW modulator.[10] A summary of the PoP experiment's parameters is listed in the righthand column of Table II.

Planned theoretical studies include beam transport simulations, sheet electron beam gun design, advanced oscillator cavity design, and additional multi-mode competition physics.

ACKNOWLEDGEMENTS

The authors would like to acknowledge technical assistance by J. Pyle. This work is supported by the U.S. Department of Energy, by SDIO/IST through a contract managed by the Harry Diamond Laboratory, and by the Office of Naval Research.

REFERENCES

1. V.L. Granatstein, W.W. Destler, and I.D. Mayergoyz, Appl. Phys. Lett. 47, 643 (1985); W.W. Destler, V.L. Granatstein, I.D. Mayergoyz, and Z. Segalov, J. Appl. Phys. 60, 521 (1986).

2. V.L. Granatstein, T.M. Antonsen, Jr., J.H. Booske, W.W. Destler, P.E. Latham, B. Levush, I.D. Mayergoyz, D.J. Radack, Z. Segalov, and A. Serbeto, Nucl. Instr. Meth. A272, 110 (1988).

3. J. Booske, A. Serbeto, T.M. Antonsen, Jr., and B. Levush, "Nonlinear Analyses for Optimized Short Period Wiggler Free Electron Laser Oscillators," to be published in Jour. Appl. Phys. (1988).

4. A. Serbeto, B. Levush, and T.M. Antonsen, Jr., Phys. Fluids, to be published (1988).

5. B. Levush and T.M. Antonsen, Jr., Nucl. Instr. Meth. A272, 375 (1988).

6. T.M. Antonsen, Jr. and B. Levush, "Mode Competition and Suppression in Free Electron Laser Oscillators," submitted for publication in Phys. Fluids (1988).

7. T.M. Antonsen, Jr. and B. Levush, "Mode Competition and Control in Free Electron Laser Oscillators," submitted for publication in Phys. Rev. Lett. (1988).

8. J.H. Booske, W.W. Destler, Z. Segalov, D.J. Radack, E.T. Rosenbury, J. Rodgers, T.M. Antonsen, Jr., V.L. Granatstein, and I.D. Mayergoyz, J. Appl. Phys. 64, 6 (1988).

9. K. Felch. Varian. personal communication (1988).

10. J. Calame. F.J. Williams. W. Lawson, and V.L. Granatstein. Bull. Amer. Phys. Soc. 31, 1601 (1986).

FIGURE CAPTIONS

Fig. 1.

FEL oscillator universal operating map. The solid lines are contours of constant universal efficiency $< \Delta P >_\chi$. The dashed lines represent equilibrium states parameterized by constant ratio of beam current to start current, $\chi = I_{beam}/I_{start}$. The dotted line delineates the region wherein stable, single-mode equilibria are possible.

Fig. 2.

Preliminary data on transmitted sheet beam current versus average wiggler field amplitude for a ten-period wiggler experiment. The shaded region indicates the measured value of injected current of approximately 18 ± A.

Fig. 3.

Geometry used for simulation of thermal analysis of short period wiggler FEL.

Fig. 4.

Temporal evolution of temperature at several representative locations within the wiggler structure. Note that for times exceeding one second. the problem becomes essentially steady state.

Fig. 5.

Maximum temperatures over the whole structure and at the cooling channels versus thermal heat flux at the cavity wall.

Table I.

$$\eta = \left(\frac{c}{\omega L}\right) \frac{(\gamma_R \beta_R)^3}{(1 + \frac{1}{2}a_{w0}^2)} \frac{< \Delta \mathcal{P} >}{(\gamma_R - 1)}, \text{ intrinsic efficiency}$$

$$P_{cav} = \left(\frac{k_z \omega}{4\pi}\right) a_{rf} b_{rf} \left(\frac{mc^2}{e}\right)^2 \left(\frac{c}{\omega}\right)^4 \frac{(\gamma_R^2 - 1)^4 \mathcal{A}^2}{L^4 a_{w0}^2 \left(1 + \frac{1}{2}a_{w0}^2\right)^2}, \text{ cavity power}^{*}$$

$$< \hat{P}_{wall} >_t \approx D \frac{(1 + r)c}{a_{rf} b_{rf} k_z} \left(\frac{\pi}{b_{rf}}\right)^2 \frac{P_{cav}}{\sqrt{2\pi\sigma\omega}}, \text{ time} - \text{averaged ohmic thermal wall flux}^{**}$$

$$I_{beam} \approx 15\lambda \left(\frac{k_z \omega}{4\pi}\right) a_{rf} b_{rf} \left(\frac{mc^2}{e}\right) \left(\frac{c}{\omega}\right)^3 \frac{(\gamma_R^2 - 1)^{5/2} T_{eff}}{L^3 a_{w0}^2 (1 + \frac{1}{2}a_{w0}^2)}, \text{ beam current}^{\dagger}$$

$$P_{out} \approx \eta \left(\frac{mc^2}{e}\right) (\gamma_R - 1)\, I_{beam} - 2 \left(\frac{\hat{P}_{wall}}{D}\right) a_{rf} L, \text{ output radiation power}$$

* - a_{rf} and b_{rf} are the long and short transverse cavity dimensions, respectively.

** - D = duty factor, r = power reflection coefficient, σ = wall electrical conductivity.

† - T_{eff} = effective cavity transmission coefficient.

Table II. Optimized FEL oscillator designs.

V_{beam} (kV)	500	410
I_{beam} (A)	60	20
b_{rf} (cm)	0.22	0.4
a_{rf} (cm)	5.0	4.0
T_{eff}	0.055	0.10
L (cm)	10.8	25.0
ℓ_w (cm)	0.54	1.0
N_w (# periods)	20	25
B_w (kG)	2.0	1.5
f (GHz)	298	120
η	0.045	0.04
$\bar{P}_{wall}$ (kW/cm^2)	2.0	0.12
P_{cav} (MW)	22.0	3.6
P_{out} (MW)	1.0	0.30

Table III. Coolant pressures to avoid boiling in channels.

Heat Load (kW/cm^2)	1000	1500	2000
Water Surface Temperature (° C)	102	144	166
Static Pressure (psig)	1	44	89
Total Input Pressure (psig)	122	165	210

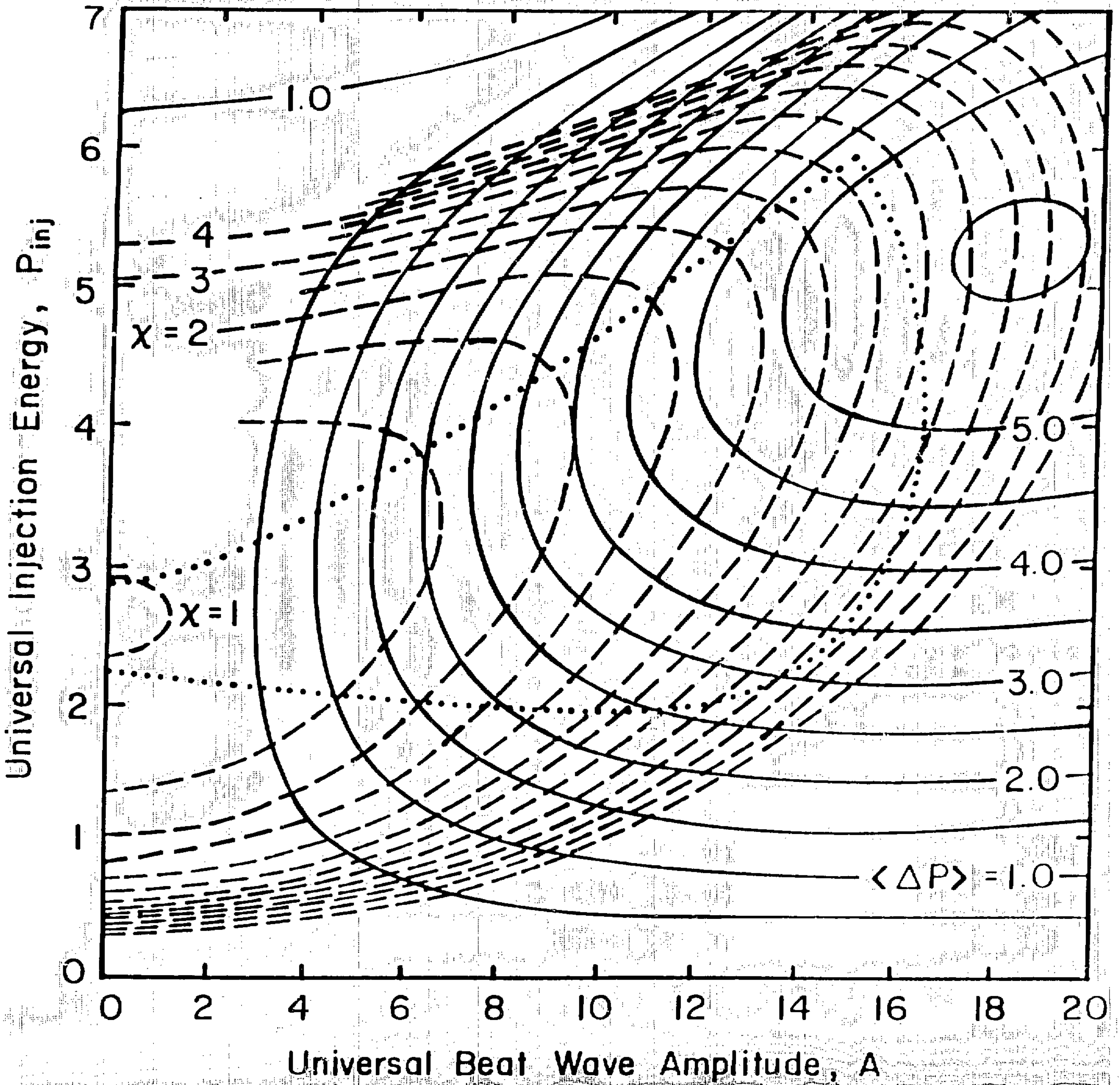
1.0
4
3
χ = 2
χ = 1
5.0
4.0
3.0
2.0
⟨ΔP⟩ = 1.0
0
1
2
3
4
5
6
7
0
2
4
6
8
10
12
14
16
18
20
Universal Injection Energy, P_{inj}
Universal Beat Wave Amplitude, A

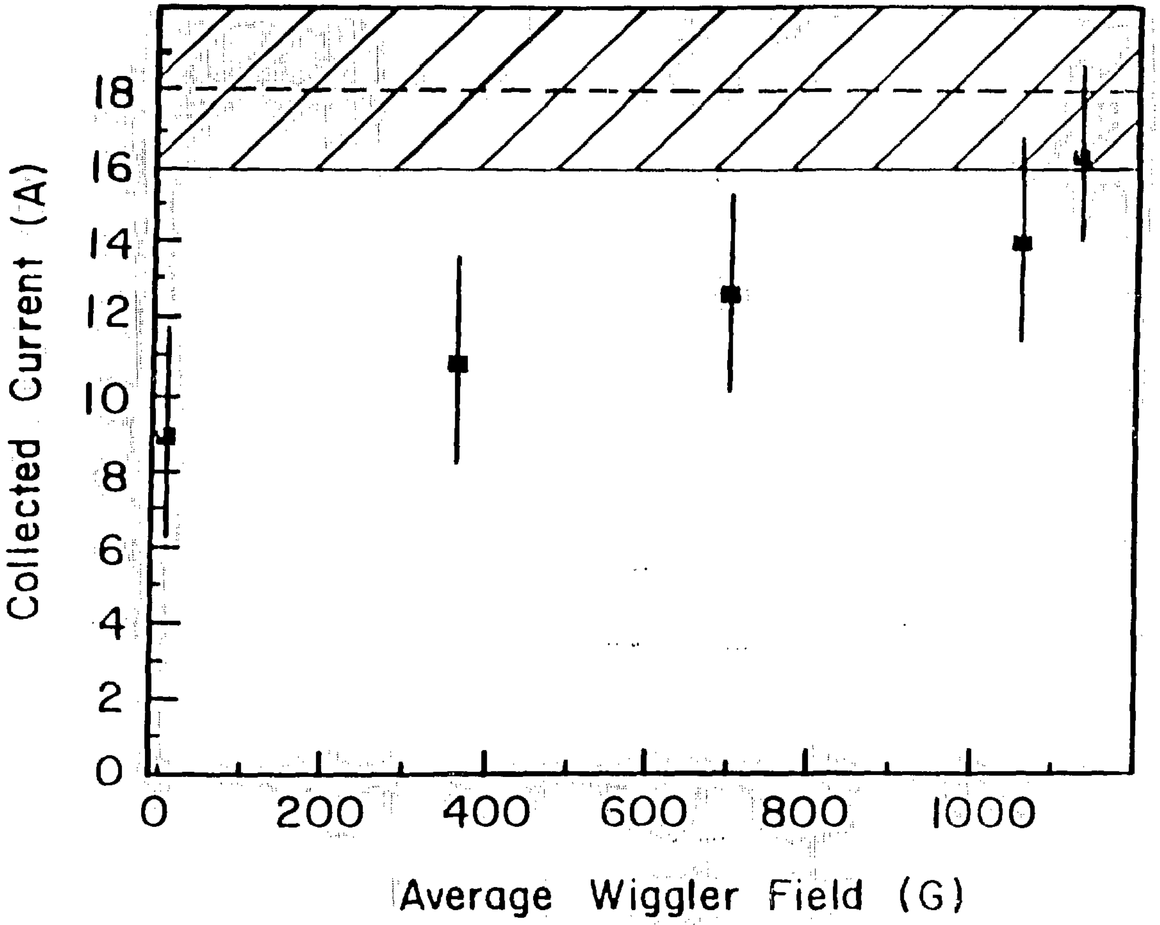
Collected Current (A)
0
2
4
6
8
10
12
14
16
18
0
200
400
600
800
1000
Average Wiggler Field (G)

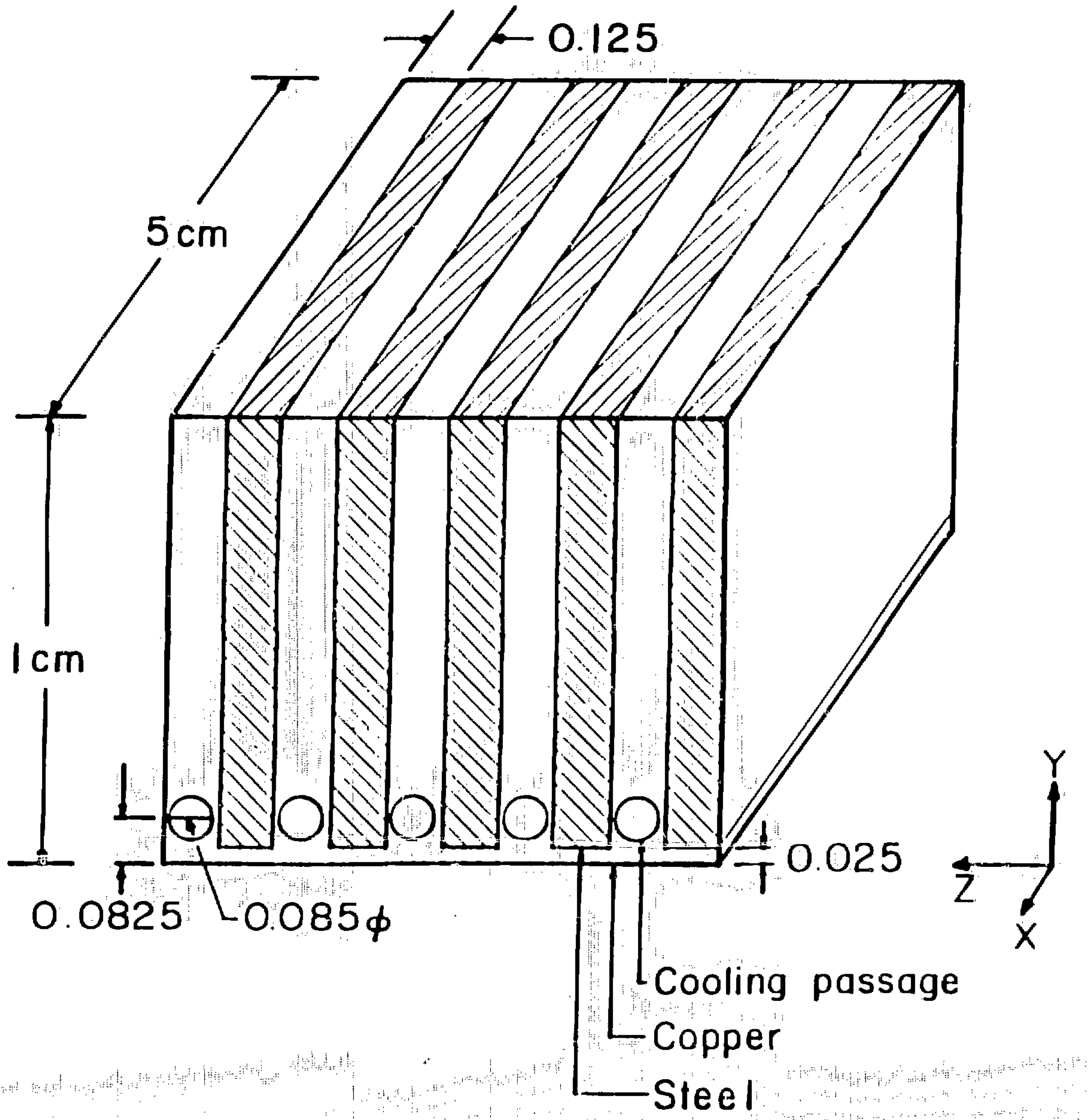

0.125
5 cm
1 cm
0.0825
0.085 φ
0.025
Y
Z
X
Cooling passage
Copper
Steel

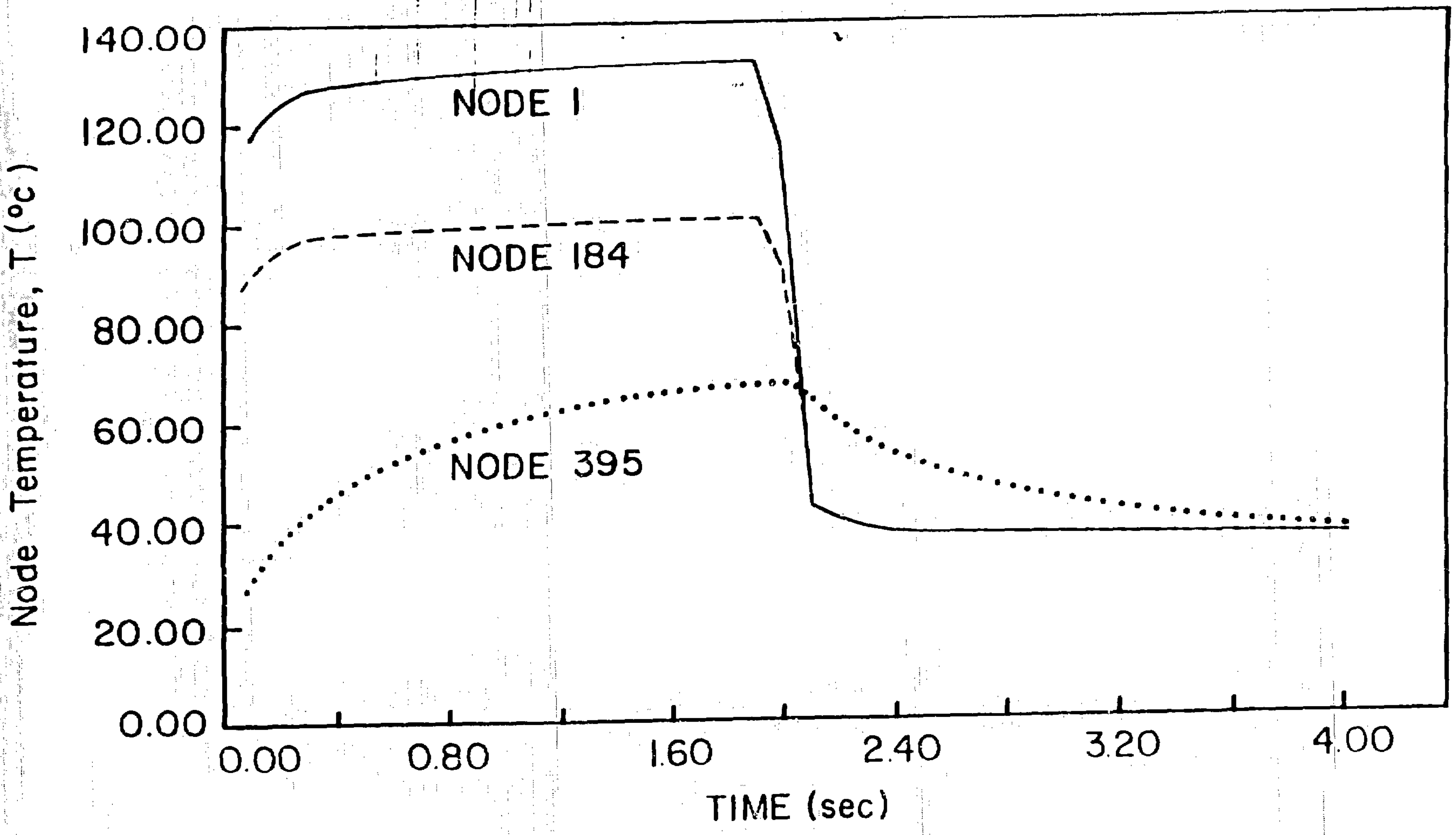

140.00
120.00
100.00
80.00
60.00
40.00
20.00
0.00
Node Temperature, T (°c)
NODE 1
NODE 184
NODE 395
0.00
0.80
1.60
2.40
3.20
4.00
TIME (sec)

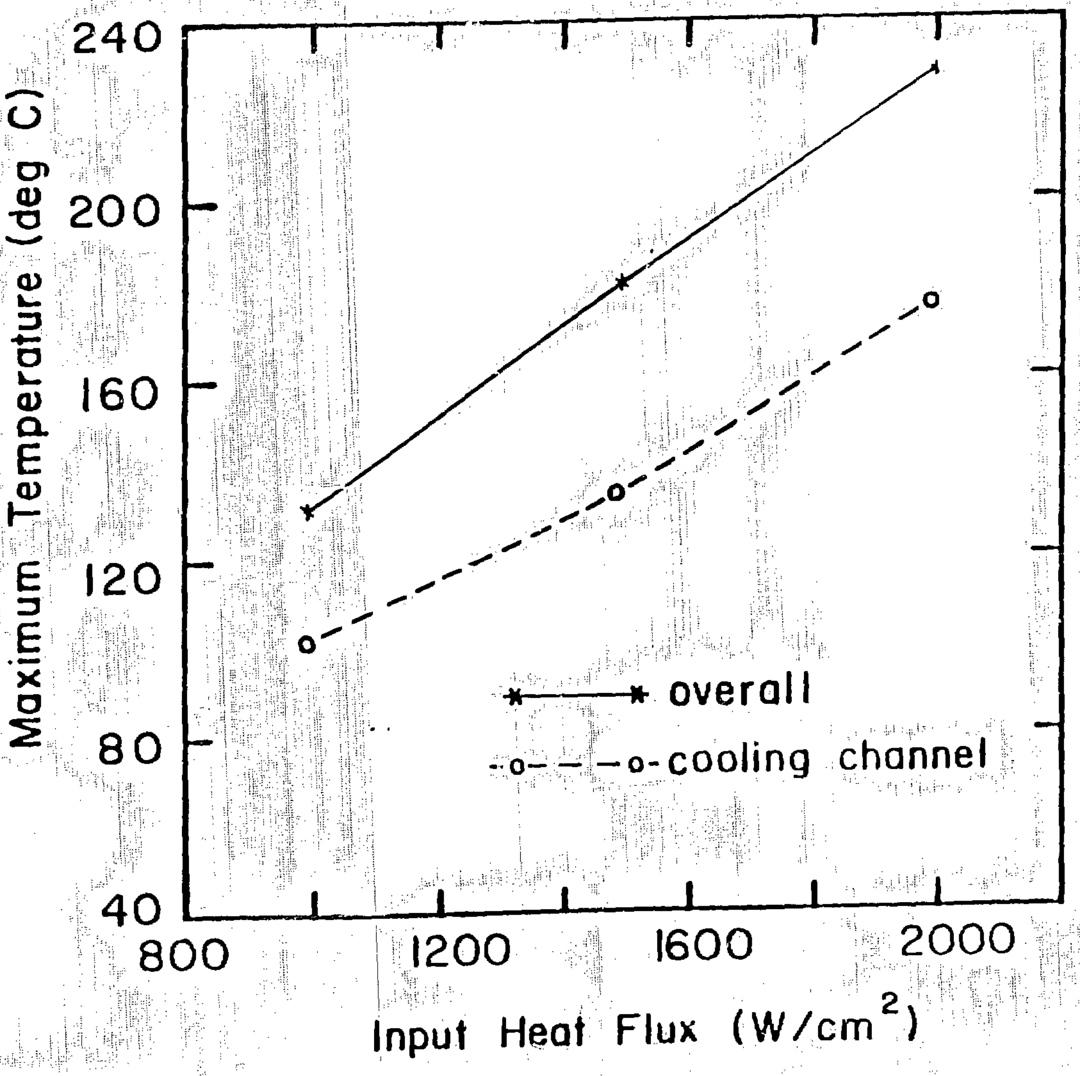
Maximum Temperature (deg C)
240
200
160
120
80
40
800
1200
1600
2000
Input Heat Flux (W/cm²)
overall
cooling channel